

# SUPPLEMENTARY MATERIAL

## S1. Additional methodological figures (uncorrected LSR' and software framework)

In short, land returns shown in black color below is consistently one order stronger (ranging from 0.00 to 0.05) than ocean returns in subtropical and tropical regions shown in magenta color (always  $< 0.005$ ). Since sea ice flag is not included in surface flag of L1B Aeolus data, high latitude water cases contain sea ice instances, leading to high OSR values (0.00 – 0.03). As seen, the ocean regions without sea/ice outside high latitudes constitute only a tiny fraction among all observations. As mentioned in the main text, this is plausible from the official Aeolus ground bin detection approach. In most cases, ocean returns do not qualify We discuss the presence of snow in details in the main manuscript. Note that the cases shown below are only illustrative and include not only surface return effects, but also atmospheric effects that are alleviated further.

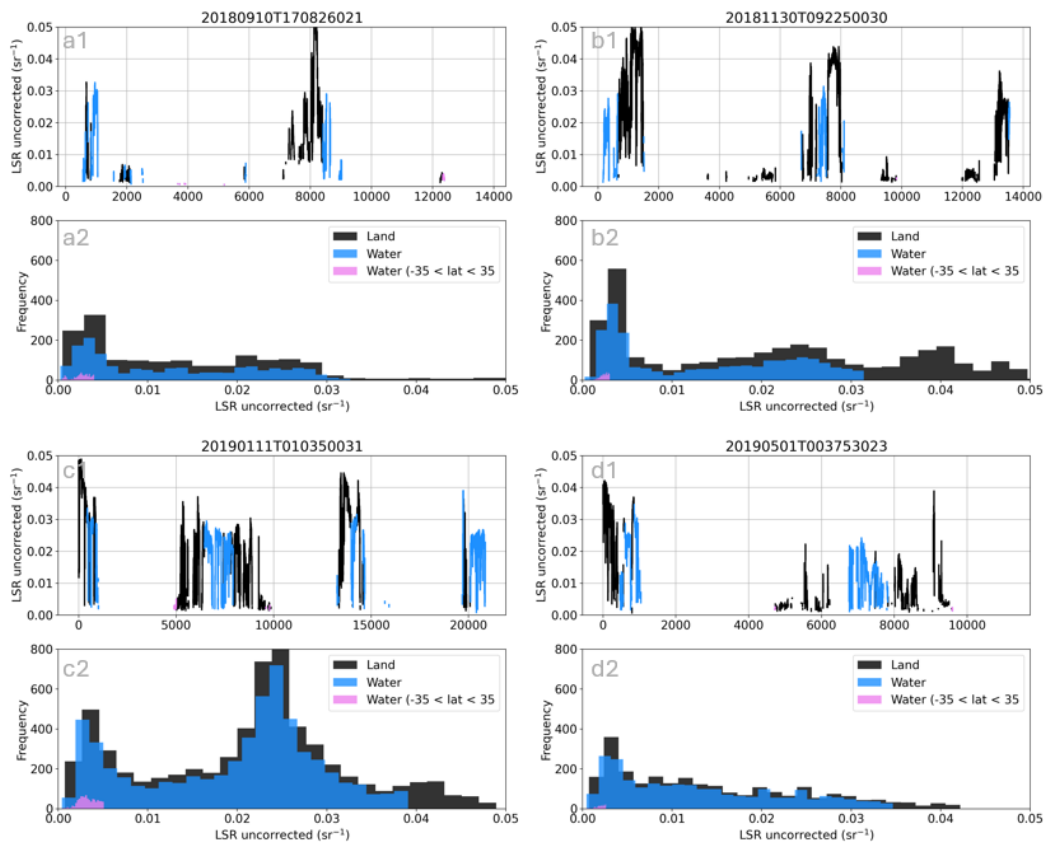
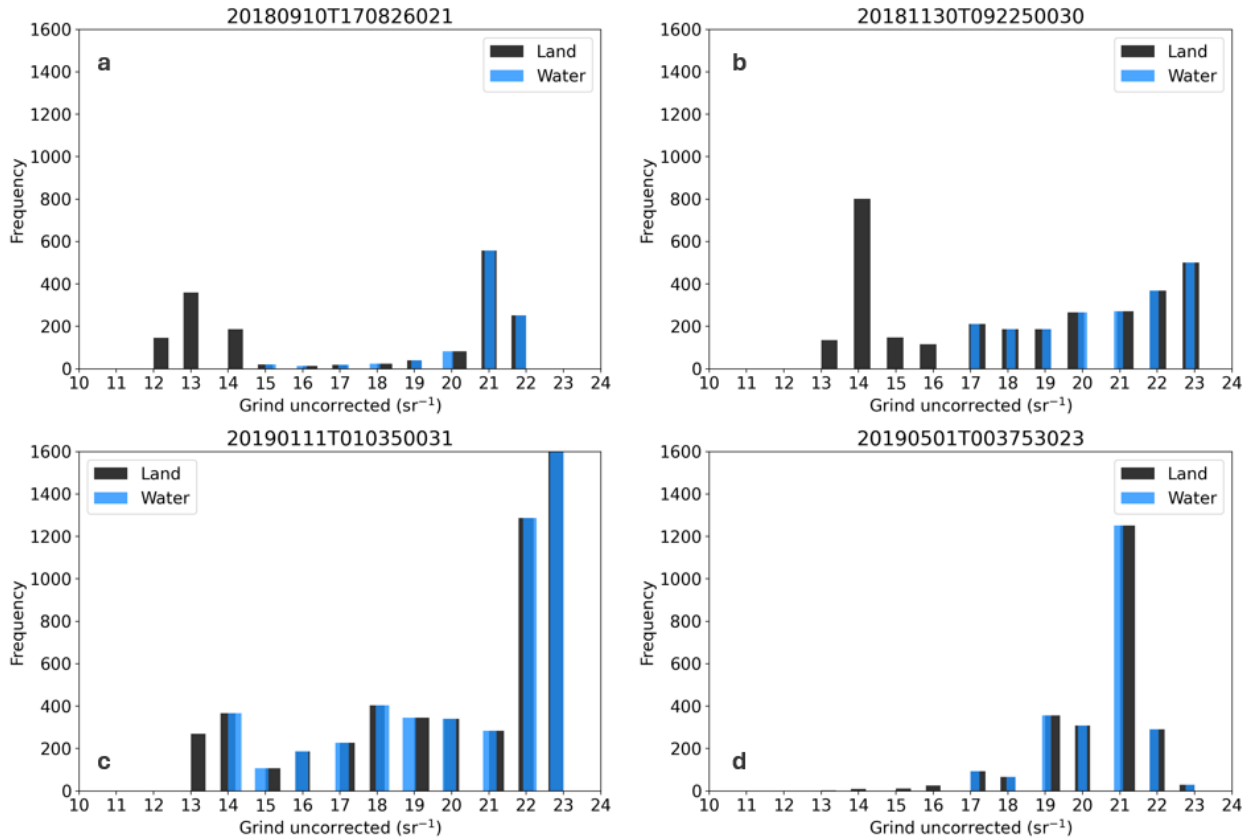
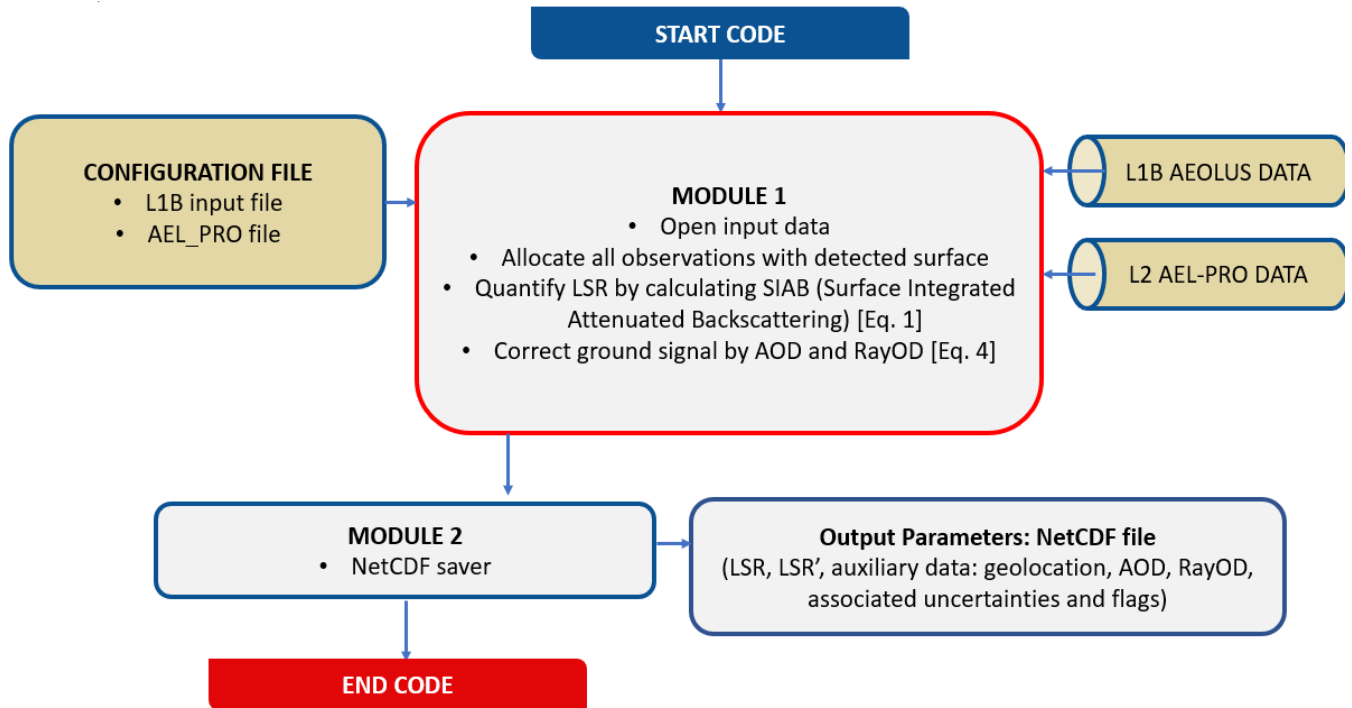


Fig. S.1 Uncorrected LSR (LSR') signal strength plots (panels with marker '1') and histograms (marker '2') shown for the reference orbits we used including: 2018.09.10 (a1, a2), 2018.11.30 (b1, b2), 2019.01.11 (c1, c2) and 2019.05.01 (d1, d2).



19  
 20 Fig. S.2 The lowest bin in lidar range gate (we count from the top to bottom in vertical dimension here) where  
 21 ground bin was detected for the reference orbits: 2018.09.10 (a), 2018.11.30 (b), 2019.01.11 (c) and 2019.05.01 (d).  
 22

23 We illustrate below the logic of the LSR software in Fig. S.3. The LSR software consists of two modules including  
 24 Module 1 that opens the Aeolus input data, allocates all observations with detected surface, quantify LSR for each  
 25 observation and correct ground signal by applying AOD and RayOD as shown in Eq. 4. Module 2 creates the output  
 26 data with LSR estimates at the given Aeolus resolution (measurement or observation, depending on the setting)  
 27 alongside associated uncertainties, auxiliary data might be required for diagnostic purposes (LSR', AOD, RayOD  
 28 etc), geolocation data and quality flags. The quality flags are used in this paper to produce attenuation-free LSR  
 29 product. These flags are described in the main manuscript text. Although the original output of Module 2 represents  
 30 all LSR estimates with detected ground bins at the original Aeolus observation, for the scientific evaluation, in this  
 31 paper we also used quality-assured LSR product after applying quality flags and gridded LSR product. The LSR  
 32 gridded product is not the part of the official Aeolus product at the moment. Note that we had previously  
 33 demonstrated that exactly the very gridded product has good agreement with passive remote sensing, sensitive to  
 34 land cover change and might be therefore very useful for scientific purposes [Labzovskii et al., 2023]. We  
 35 emphasize that the software is now being developed and will be available in the prototype version before the official  
 36 Aeolus Phase-F release.

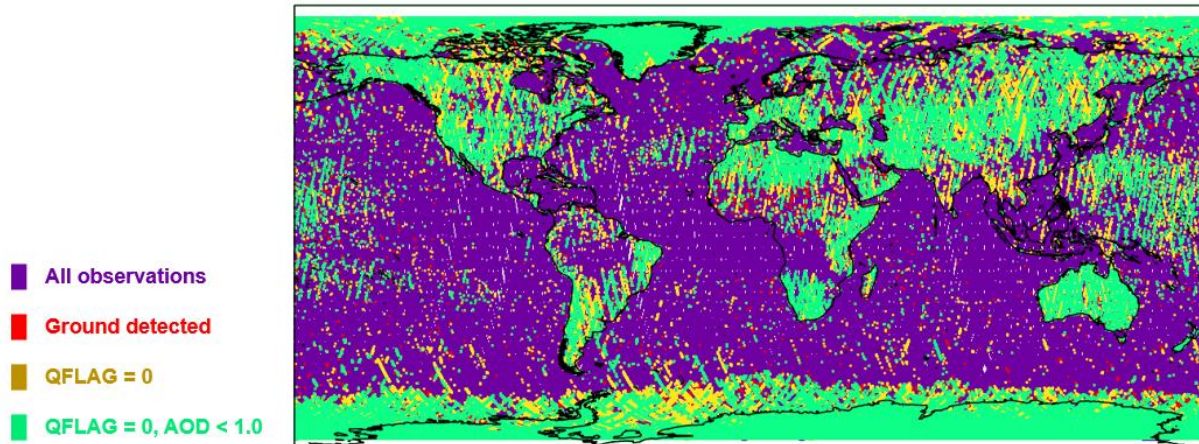


38  
39 Fig. S3. Schematic representation of the LSR algorithm as to be implemented within the L2A Aeolus product  
40

41  
42 **S2. Filtering out attenuated LSR observations**

43 In this section, we illustrate some examples of LSR observations cleaned and not cleaned by applying ‘qflag’ or  
44 Aeolus quality flag described in the main manuscript. Fig. S4 below shows Aeolus LSR observations from  
45 September 2018 with all unfiltered observations (violet), only observations where ground bin was located by the  
46 official algorithm (red), observations with qflag = 0 (yellow) and observations with qflag = 0, AOD < 1.0. We call  
47 these observations “clear” in the main manuscript. As seen, the number of clear observations can dramatically differ  
48 depending on the strategy. The observations shown in violet are not useful because they do not contain any ground  
49 detection signal according to the official surface detection algorithm. They only illustrate the total number of  
50 available orbits with observations, not of which can be applied for the LSR retrieval. There is no visible difference  
51 between red-colored observations, which contain ground detection signal and those observations we marked as  
52 attenuation free by yellow color. In other words, the official ground detection algorithm works approximately nearly  
53 as effective as the qflag-based filtering of attenuative features introduced in our previous work [Labzovskii et al.  
54 2023] about Aeolus LSR. Green-colored observations in Figure S1 represent clear, final LSR estimates that are used  
55 in the final analysis for September 2018. For other months, we use the same procedure to produce clearest LSR  
56 observations.

LSR observations using different filtering strategies | September 2018



58  
59

60 Fig. S.4 Aeolus LSR observations from September 2018 with all unfiltered observations (violet), only observations  
61 where ground bin was located by the official algorithm (red), observations with qflag = 0 (yellow) and observations  
62 with qflag = 0, AOD < 1.0.

63

64 For clarity, we quantified the number clear (e.g. green-colored) observations used in the final analysis in Table S2  
65 below. As expected, for all months, only some fraction of Aeolus LSR observations contain ground signal (see  
66 column ‘Ground Detected’ in Table S2 below. In percentage, the number of observations containing ground ranges  
67 from 8% (September 2018) to 22% (January 2019) during FM-A period from the total number of observations. As  
68 seen, in absolute terms, these numbers correspond to the range of 465,044 – 1,132,018 ground-containing  
69 observations per months. Among these observations with ground signal within, the majority of observations passed  
70 the aforementioned criteria to be considered clear. The number of clear observations per month range from 366,529  
71 (September 2018) to 1,026,869 (March 2019) during FM-A period.

72

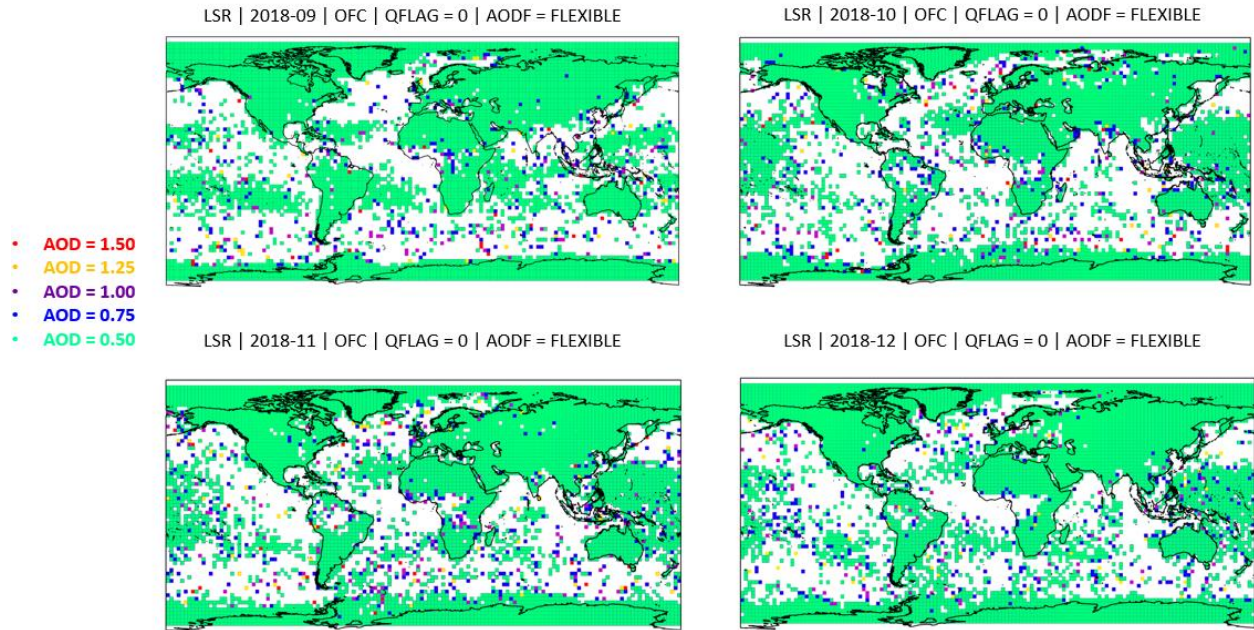
73 Table S.2 Statistics on the LSR data abundance for FM-A period.

74

date	All	Ground Detected (GD)	GD & qflag = 0	GD & qflag = 0 & AOD < 1
2018/09	5,480,310	465,044	393,218	366,529
2018/10	6,398,400	645,696	520,056	482,108
2018/11	5,937,690	1,115,751	874,464	808,765
2018/12	6,213,600	1,255,028	972,504	898,912
2019/01	2,760,390	605,257	470,673	436,531
2019/02	2,659,800	520,681	359,191	330,899
2019/03	6,512,100	1,324,018	1,128,701	1,026,869
2019/04	6,263,430	1,168,668	949,454	859,650
2019/05	6,507,330	959,369	728,891	660,989

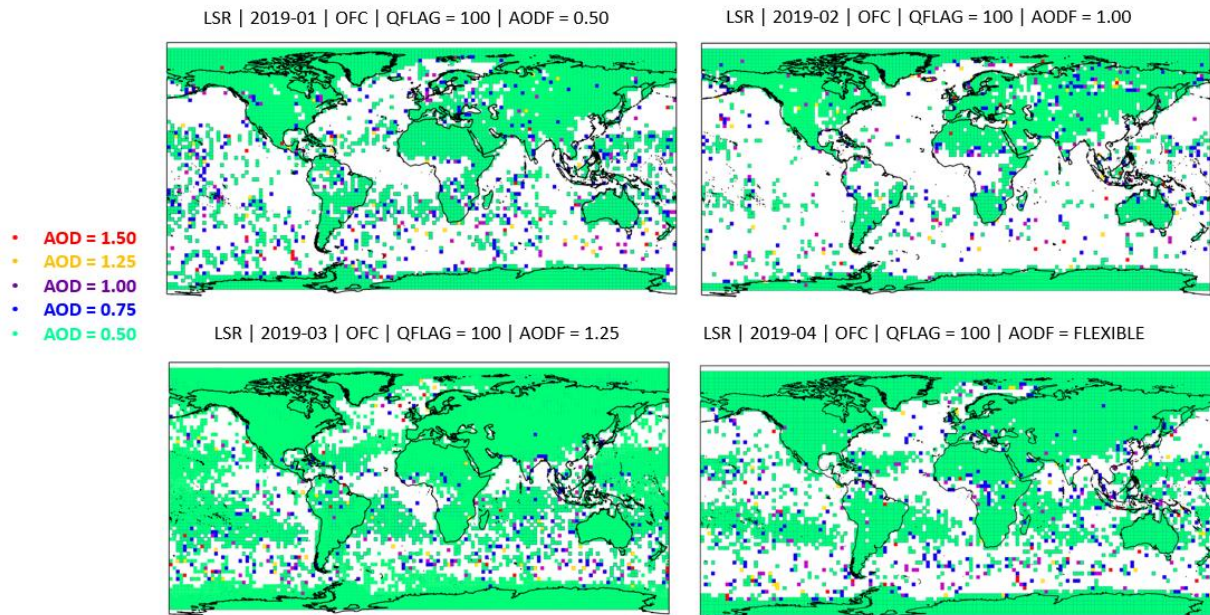
75

76 To ensure a stability of LSR retrieval to attenuative feature filtering strategies, we illustrate Fig S3 below. It shows  
77 the difference between original strategy of AOD-based filtering of LSR. To remind, Fig. 2 in the main text shows a  
78 procedure of filtering out attenuated LSRs. The step 2 on Fig. 2 includes the point of filtering out aerosol-attenuated  
79 cases of LSR detection at the threshold of  $AOD = 1.0$ . In other words, for gridding, all the LSR values  
80 corresponding to  $AOD > 1.0$  values are filtered out from the analysis. Since this choice is rather arbitrary and comes  
81 from the experience of our previous study [Labzovskii et al., 2023], here we tested the sensitivity of LSR to this  
82 AOD threshold. Ideally, LSR should not be very sensitive to minor changes in AOD thresholding. The reasons are:  
83 (1) we should have enough clear observations per each grid cell to calculate LSR means and (2) most attenuated  
84 signals are filtered out at the quality flag checking stage. Thus, AOD filtering ensures that we not include some  
85 possibly wrong retrieval values and we do not bias our results towards weaker LSR in the regions, where AOD  
86 might be high (in this case, LSR is being attenuated not due to the surface reflectivity effects, but due to atmospheric  
87 effects). Due to this, we quickly tested the difference in LSR data abundance depending on the flexible AOD  
88 threshold for the Aeolus FM-A period (see Fig-s S4 and S5 below). We calculated averaged LSR estimates at  $2.5 \times$   
89  $2.5$  resolution with different thresholds. We found only a minor difference in LSR estimates between various AOD  
90 thresholds (0.50, 0.75, 1.00, 1.25, 1.50). Interestingly, despite the large difference between highest (1.50) and the  
91 lowest threshold (0.50), the data availability hardly varies mostly over water where signal is weak. For instance, in  
92 2018/09 our selected threshold of AOD of 1.00 results in 5 221 grid cells. At the same time, lowering the threshold  
93 only slightly affects LSR grid estimate abundance by lowering the amount of cells down to 5 121 at 0.75 and to 4  
94 806 at 0.50 threshold. Meanwhile, raising a threshold up to 1.25 and 1.50 values yields just slightly higher number  
95 of grid cells, as said above, most found above water with 5 272 cells at 1.25 and 5 300 cells for 1.50. The differences  
96 between LSR estimates at different AOD thresholds are relatively consistent for other months as well, so we did not  
97 provide more detailed statistics here. Overall, with the OFC strategy of surface detection,  $AOD = 1.0$  seems like a  
98 reasonable choice since most attenuated cases are already filtered out at the quality flag application stage.



99  
 100 Fig S4 Sensitivity experiment using different AOD filtering strategies for September 2018, October 2018,  
 101 November 2018 and December 2018. Color denotes the maximum AOD value below which LSR was considered  
 102 completely attenuated.

103  
 104



105  
 106 Fig S5 Sensitivity experiment using different AOD filtering strategies for January 2019, February 2019, March 2019  
 107 and April 2019. Color denotes the maximum AOD value below which LSR was considered completely attenuated.

108  
 109

110 Table S.3 below is shown to familiarize a reader with a complete list of codes, denoting atmosphere features in  
 111 AEL\_FM algorithm, incorporated in the latest AEL\_PRO version.

112

113 Table S.3 List of atmospheric features according to AEL\_FM classification incorporated into AEL\_PRO dataset  
 114 used for filtering out attenuated LSR cases for the final analysis

0	Clear sky tropospheric
100	Clear sky and used in Pass1 (tropospheric)
200	Clear sky and used in Pass1 (stratospheric)
1	Water cloud
101	Water cloud and used in Pass1 (tropospheric)
201	Water cloud and used in Pass1 (stratospheric)
2	Ice cloud tropospheric
102	Ice cloud tropospheric and used in Pass 1
3	Tropospheric aerosol
103	Tropospheric aerosol and used in Pass 1
13	Stratospheric Aerosol
213	Stratospheric Aerosol and used in Pass1
11	PSC-Type 1
211	PSC-Type 1 and used in Pass1
12	PSC-Type 2
212	PSC-Type 2 and used in Pass 1
1000 >= Index <2000	Attenuated and is tropospheric
2000 >= Index <10000	Attenuated and is stratospheric
Index > 10000	Surface

115

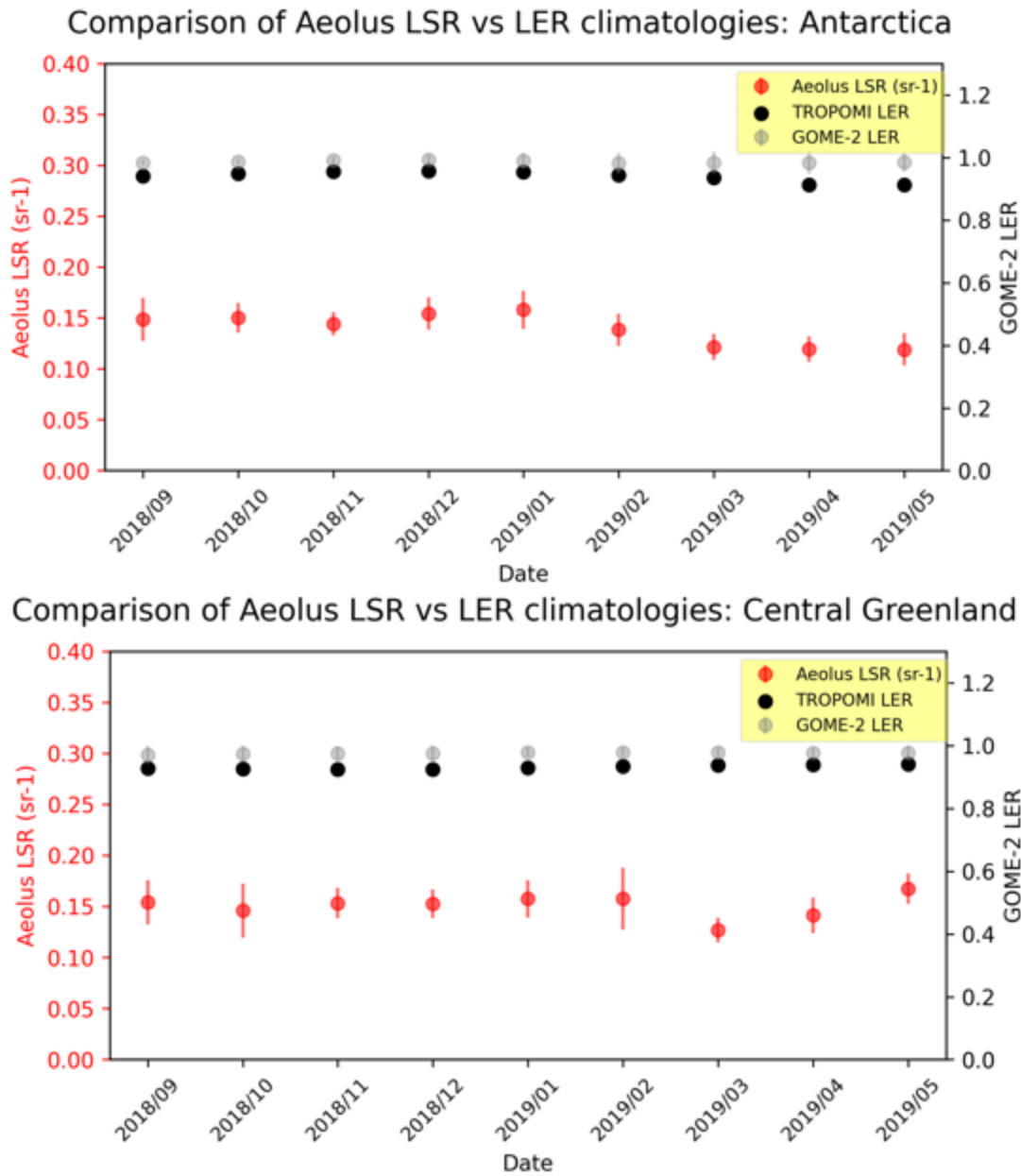
116

117

118 Below, we illustrate several additional regional figures, illustrating the regional analysis we described in section 3.3

119 To be specific, Fig. S7 shows Antarctica and Central Greenland (snow-covered regions).

120



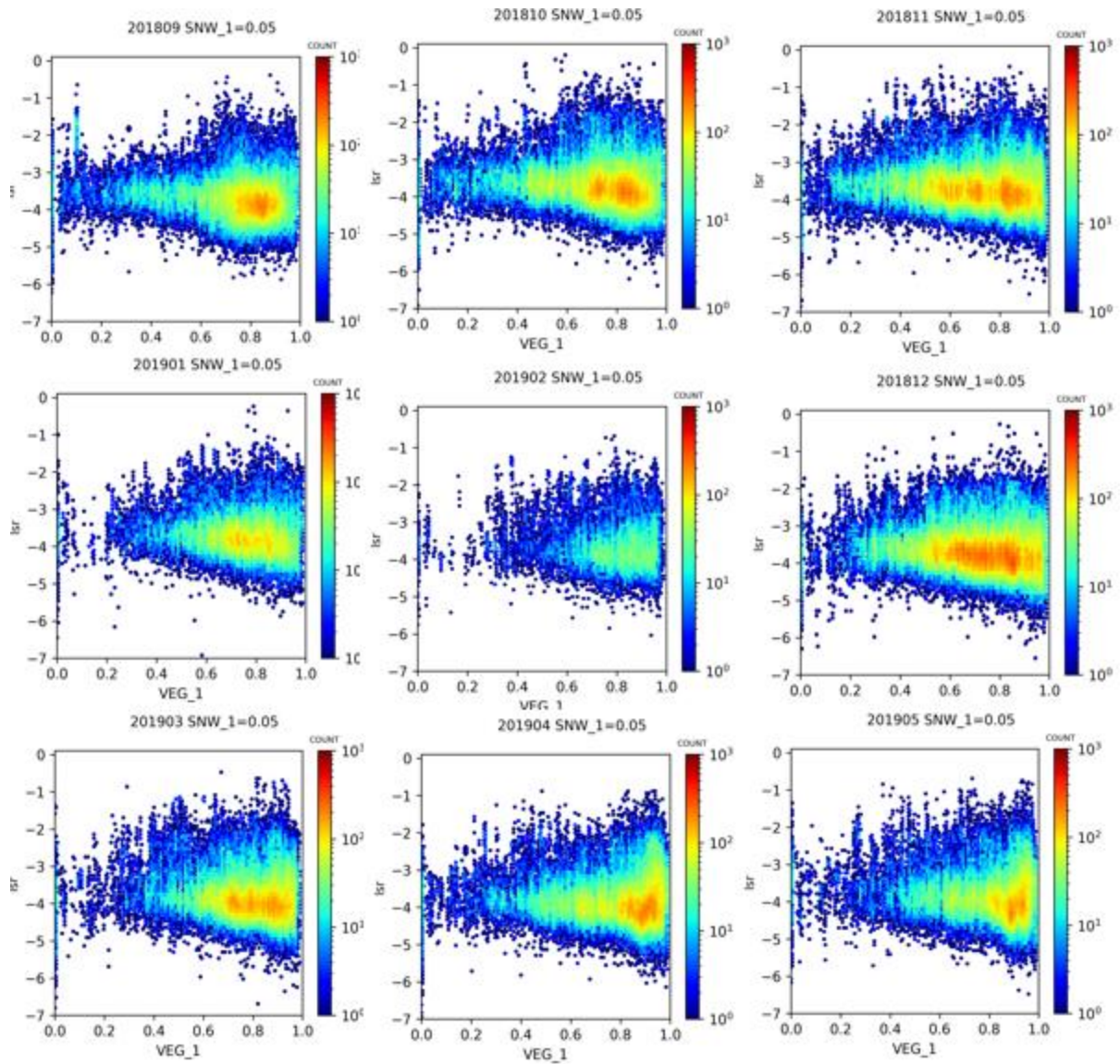
121  
 122 Fig. S7 LSR (red) comparison with LERT (black) and LERG (grey) for: a – Antarctica, b – Central Greenland. Error  
 123 bars are taken from one-sigma monthly deviations of average LSR.

124

125

126 Below, we demonstrate another version of Fig. 17 illustrating scatterplots between LSR and NDVI, but with snow  
 127 cover values of  $> 0.05$  being filtered out. In other words, this is a figure, illustrating pure LSR – NDVI comparison.





128

129

130

131

132

133

Fig. S8 Monthly scatterplots comparing LSR (sr-1) and NDVI (VEG\_1) for the entire FM-A period. Y-axis and colorbar are both shown in logarithmic scales. Snow cover mask applied, whereas all observations corresponding to snow cover > 0.05 are filtered out from the analysis.